

Electric-field modification of magnetism in a thin CoPd film

Mikhail Zhernenkov, M. R. Fitzsimmons, Jerzy Chlistunoff, and Jaroslaw Majewski
Los Alamos National Laboratory, Los Alamos, New Mexico 87545, USA

Ioan Tudosa and E. E. Fullerton

University of California, Center for Magnetic Recording Research, San Diego, La Jolla, California 92093, USA

(Received 8 June 2010; revised manuscript received 25 June 2010; published 20 July 2010)

We report the modification of the magnetization depth profile of an 18.5-nm-thick Co₅₀Pd₅₀ film immersed in an electrolyte using an electric field. We find an increase in the surface magnetization that varies linearly with magnitude of the applied potential. The change in magnetization occurs within 7.2 nm of the CoPd surface.

DOI: 10.1103/PhysRevB.82.024420

PACS number(s): 75.70.Cn, 61.05.fj, 75.80.+q, 85.75.-d

I. INTRODUCTION

In the last several years spin electronics has developed into a vibrant field of science and technology due to the strong interplay of electric current and magnetism at nanometer length scales.¹ Examples include giant and tunnel magnetoresistance sensors used in magnetic read-heads. The use of an electric field (E) to actuate a magnetic response is not widespread and has until recently been limited to materials with low Curie temperatures (T_C) (Refs. 2 and 3) or to low temperatures at which the effect is observable^{4,5} or to the weak interaction between electric field and magnetism.⁶ T_C of 3d transition metals and their alloys can be well above room temperature;⁷ however, these materials are conductors so the influence of E fields on magnetism is severely constrained.⁸⁻¹⁰ Despite these difficulties, control of magnetism with E fields is attractive, because E fields can be localized to nanometer length scales and often require less energy to produce than magnetic fields.

An experimental approach to directly influence surface magnetism with E fields is to use an electrochemical cell.^{11,12} When a negative potential is applied to a metal (ferromagnet, in our case) electrode in an electrochemical cell, the metal surface is charged with excess electrons. The charge is counterbalanced by cations from the electrolyte solution, which collect predominantly at the electrode surface and form an insulating ionic layer (double layer). This phenomenon produces a large electric field at the interface. The electric field is uniform for flat and smooth surfaces, such as those required for neutron-scattering experiments.¹³

The electric field may affect the surface magnetization in two ways. First, the E field may shift the Fermi level ε_F , and change the densities of the state (DOSs) of spin-up and spin-down electrons at ε_F . Since the difference between the DOS for spin-up and spin-down electrons integrated over the band to ε_F [namely, green (right) and red (left) areas in Fig. 1] is the net magnetization,¹³⁻¹⁸ a change in ε_F may increase or decrease the magnetization.¹⁸ The change in the magnetization δM when ε_F is perturbed is: $\delta M \sim [D^\uparrow(\varepsilon_F) - D^\downarrow(\varepsilon_F)] \frac{\partial \varepsilon_F}{\partial E} \delta E$, where $D^{\uparrow\downarrow}(\varepsilon_F)$ are spin-up or spin-down DOS of electrons at ε_F and δE is the change in applied electric field. A second effect of an E field may be to change the orbital occupancy, e.g., from $d_{3z^2-r^2}$ to $d_{x^2-y^2}$, thus, modifying the magnetic anisotropy of the film.¹⁹

Recently, the influence of an E field on the magnetic anisotropy of ordered FePt and FePd thin films was reported.¹³ This influence was measured by polar Kerr spectroscopy at room temperature. The largest changes in coercivity, -4.5% for the 2-nm-thick FePt film and $+1\%$ for the 2-nm-thick FePd film, were observed for the largest applied potential from which an E -field-induced change in magnetic anisotropy was inferred. In addition, a 3% change in Kerr angle was detected for the 2-nm-thick FePt film, which is consistent with a change in magnetization. The fractional change in coercivity for the 2-nm-thick films was reported to be larger than for the 4-nm-thick films. This observation is consistent with the notion that the E field preferentially modifies the surface magnetization. However, Kerr spectroscopy is not able to provide the magnetization depth profile nor can it provide a quantitative measure of magnetization. Here, we report results of a polarized neutron reflectometry (PNR)

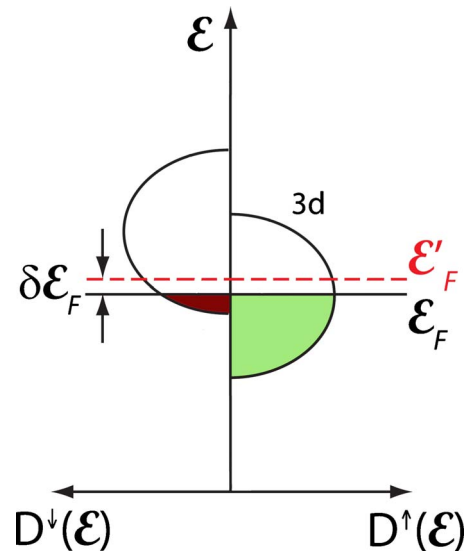


FIG. 1. (Color online) Illustration of the density of states $D^{\uparrow\downarrow}(\varepsilon_F)$ of a ferromagnet near the Fermi level ε_F (Ref. 18). Difference of $D^{\uparrow\downarrow}(\varepsilon_F)$ integrated from the bottom of the band to ε_F is the net (spin) magnetization. The integrated DOS for spin-up and spin-down electrons are shown by green (right) and red (left) areas, accordingly. Shift of ε_F to ε'_F changes the green and red integrals differently, thus changing the magnetization.

study in which we quantitatively measured an enhancement of magnetization (i.e., δM as opposed to anisotropy) due to E fields and the depth of the perturbed magnetization from the sample surface.

II. SAMPLE CHARACTERIZATION

An 18.5-nm-thick $\text{Co}_{50}\text{Pd}_{50}$ film was deposited by magnetron sputtering on a single-crystal quartz substrate first covered with a 4.7-nm-thick polycrystalline buffer layer of Ta. Magnetometry confirmed that the anisotropy of the film was in the sample plane. The magnetization was easily saturated by the 3 kOe magnetic field applied in the sample plane during the neutron experiments. Chemical analysis of the electrolyte (propylene carbonate, PC) performed after the neutron experiment detected Pd and Co corresponding to a loss of 3% Pd and 0.5% Co from the sample. We attribute small losses of Pd and Co from the film to corrosion of the sample (despite the good corrosion resistance of CoPd alloys²⁰) once it was immersed in the electrolyte. Some corrosion was believed to have occurred before application of the negative potential during the neutron experiment. A negative potential inhibits chemical attack of the CoPd film.²¹

III. EXPERIMENTAL TECHNIQUE

PNR involves the specular reflection of a polarized neutron beam from a magnetized surface or film.^{22–24} The intensity of the specularly reflected radiation is measured as a function of wave-vector transfer Q (equal to the magnitude of the difference between incoming and outgoing wave vectors) and beam polarization with respect to the applied magnetic field. PNR provides both nuclear (chemical) Nb and magnetic Np , scattering length density (SLD) depth profiles of the sample averaged over the coherent region of the neutron beam on the sample surface—typically square micron.²⁵ N refers to the number density of atoms and b and p are their nuclear and magnetic scattering lengths, respectively. The spin dependence of the scattering stems from the two neutron-scattering lengths, $b^\pm = (b \pm p)$, where the sign of the term corresponds to the measured reflectivities R^\pm when the polarization vector of incident neutron beam is parallel (+) or antiparallel (–) to the external magnetic field. The magnetic SLD Np of the sample is directly proportional to magnetization through the coefficient $2.853 \times 10^{-9} \text{ \AA}^{-2} \text{ cm}^3/\text{emu}$.

IV. RESULTS FROM THE NEUTRON-SCATTERING EXPERIMENT

The first neutron reflectivity measurement was of the virgin sample in the absence of the electrolyte. The remaining measurements were taken with the electrolyte as a function of dc potential. The dc potential was applied by a potentiostat between the working electrode (the CoPd film in contact with the electrolyte solution) and a counter electrode (a large stainless steel plate covered with a 500-nm-thick Pt layer) (Fig. 2). The reference electrode was immersed in the electrolyte between the working and counter electrodes.²⁶ PNR data were taken at room temperature for three values of applied potential U in the sequence: -0.32 , -0.15 , and

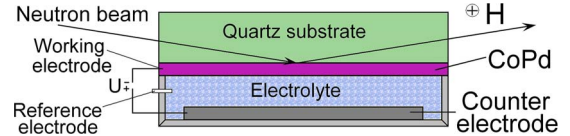


FIG. 2. (Color online) Schematic of the electrochemical cell. A 3 kOe field was parallel to the sample surface; E field was obtained by applied potential U measured against reference electrode.

-0.02 V measured relative to the reference electrode. The data have been corrected for the imperfect polarization of the neutron beam and wavelength variation in the neutron spectrum.

Once immersed in an electrolyte solution, an ionic insulating layer is expected to grow on the sample's surface.¹³ The insulating layer (which is needed in order for an E field to be applied to the sample) affects the reflectivity of the sample compared to its virgin state. We collected a series of reflectivity measurements shortly after the sample was immersed in the electrolyte with an applied potential of -0.32 V. During the subsequent 30 h, the sample reflectivity changed (Fig. 3). Analysis of the PNR data (discussed later) indicated that the change in the sample's reflectivity was consistent with growth of an organic layer (see also Ref. 13). After 30 h (Fig. 3 green circles), the reflectivity no longer changed with time. Thus, the chemical structures of the sample and the organic insulating layer no longer changed with time. Once the reflectivity no longer changed, we collected the reflectivity curve for $U = -0.32$ V. During measurements at other applied potentials, we verified that the reflectivity did not change with time. Some of these control measurements are shown in Fig. 3. The similarity of the control measurements taken after 30 h (Fig. 3) supports our conclusion that the sample's chemical structure (and attendant organic layer) did not change during the measurements of the data at different applied potentials.

The neutron reflectivities R^+ and R^- for the virgin sample in the absence of the electrolyte are shown in the Fig. 4(a). The normalized spin difference (NSD) curve shown in Fig. 4(b) is given by $\frac{(R^+ - R^-)}{R_F}$, where $R_F = \frac{16\pi^2}{Q^4}$ is the Fresnel coefficient. The NSD data corresponding to different values of

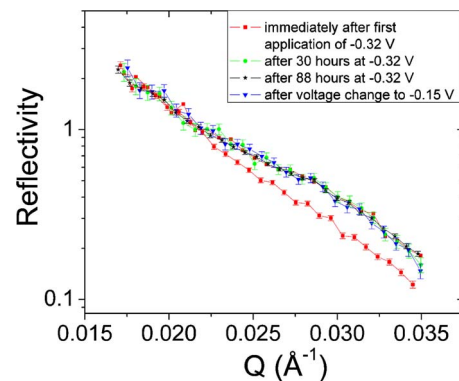


FIG. 3. (Color online) Control measurements to monitor the time dependence of the change in the sample's reflectivity. Measurements shown in Fig. 4 were taken after the sample's reflectivity no longer changed with time.

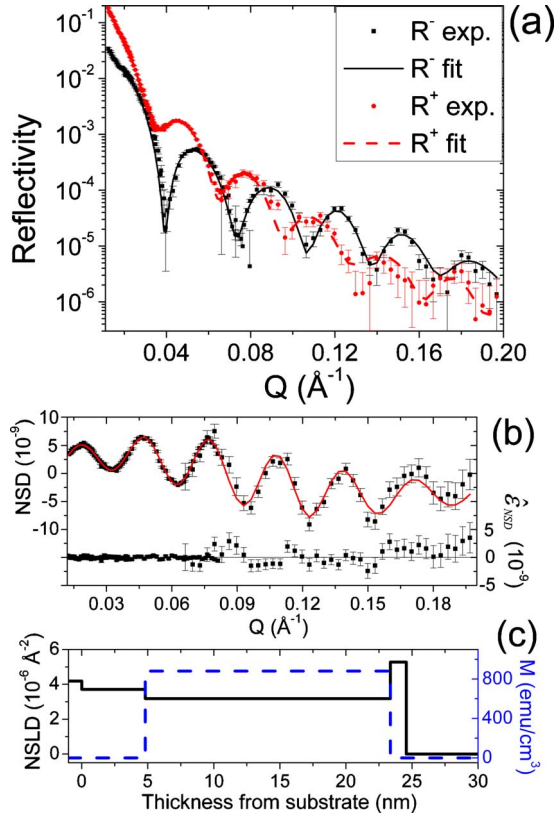


FIG. 4. (Color online) (a) Reflectivity data taken without electrolyte. Solid black and dashed red curves represent the fit to the data. (b) NSD data, the fitted curve (solid curve), and the NSD residuals $\hat{\epsilon}_{\text{NSD}}$; (c) variation in the model parameters for the nuclear (black line is the “NSLD”) and magnetic (dashed blue line is M) SLDs used to produce the curves in figures (a) and (b).

applied potential are shown in Fig. 5. The amplitude and period of the oscillatory variation in the NSD (there may be a superposition of oscillatory variations with different periods) are related to changes in the SLD across interfaces and the separation of the interfaces.²⁷

V. DISCUSSION

In order to quantify the influence of the E field on the CoPd magnetization, we used the dynamical formalism of Parratt²⁸ to calculate R^{\pm} for a simple model for the nuclear and magnetic SLD profile of the sample. The chemical profile of the film, including the surface and interface roughness and film thickness, was obtained from a fit to the data taken from the sample in the virgin state. We used the literature SLD values for the substrate, Ta layer and $\text{Co}_{50}\text{Pd}_{50}$ alloy, and refined the layer thicknesses, interface roughness (or interdiffusion) and magnetization of the CoPd film. The fitting process involved optimizing the model parameters to obtain the minimum of χ^2 —a measure of goodness of fit.²⁹ Errors reported for these parameters represent the perturbation of a parameter that increased χ^2 by the number four which corresponds to a 2σ error (95% confidence).²⁹ The chemical and magnetic depth profiles yielding the best fit are shown in Fig. 4(c). The thicknesses of the Ta and CoPd layers were 4.7(1)

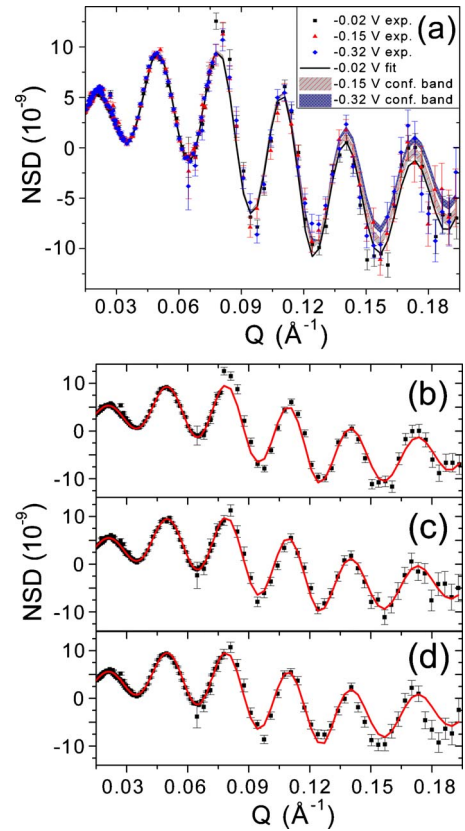


FIG. 5. (Color online) (a) NSD data for different applied potentials and fits to the data. The 95% confidence bands are shown. These bands do not overlap at high Q . [(b)–(d)] NSD data and the fitted curves (solid red lines) for $U=-0.02$ V, $U=-0.15$ V, and $U=-0.32$ V, respectively.

nm and 18.5(1) nm, respectively. Notably, a thin 1.5(1) nm Co-(mono)oxide layer was detected on top of the CoPd alloy film which can be explained by natural oxidation of Co.³⁰ The magnetic SLD Np was determined to be $(2.51 \pm 0.01) \times 10^{-6} \text{ \AA}^{-2}$ which corresponds to the unperturbed CoPd film bulk magnetization $M_v(z)=880 \pm 4 \text{ emu/cm}^3$ and is in good agreement with magnetometry measurements.

The fitting procedure for the film in contact with electrolyte consisted of fitting a model to the R^+ and R^- [solid black and dashed red curves, Fig. 4(a)] and optimizing the χ^2 metric to the NSD curves [Figs. 5(b)–5(d)]. For the reflectivity data taken for $U=-0.02$ V nuclear and magnetic SLDs of the CoPd layer were equal to those of the virgin sample and the four adjustable parameters were optimized: the thickness of the CoPd layer, the thickness of the layer “3,” its nuclear SLD and its roughness. We found the only difference between the chemical structures of the CoPd film for the virgin sample and the CoPd film after immersion in the electrolyte was a 0.2(1) nm reduction in the CoPd film thickness. The reduction in CoPd film thickness is consistent with the amount of Co and Pd detected in the electrolyte from our chemical analysis. The model and the NSD fitting curve are shown in Figs. 4(b) and 6(b), respectively. This result for the case of -0.02 V corresponds to a reduced $\chi^2_v=2.7$ (i.e., χ^2 divided by the number of data points less the number of optimized parameters). The nuclear SLD of layer 3 is con-

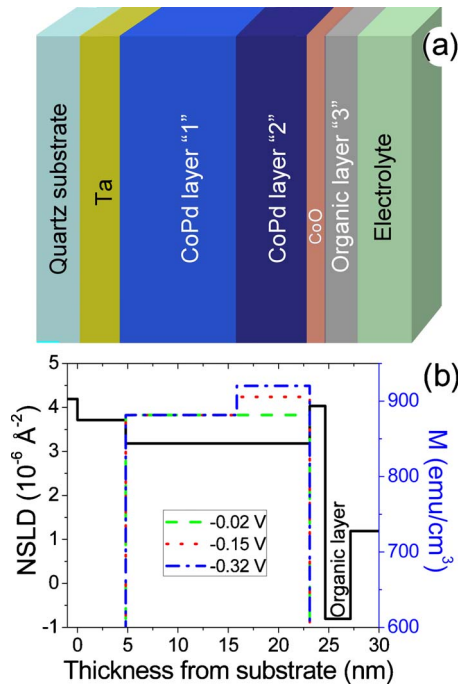


FIG. 6. (Color online) (a) Schematic of the model to fit the data. (b) Variation in the model parameters (dashed green, dotted red, and dashed dotted blue lines) corresponding to (a) for the magnetization of CoPd film as a function of U (associated with “ M ” scale) and nuclear SLD (the solid black line associated with NSLD scale). The nuclear SLD is the same for all three measurements.

sistent with the presence of organic material on the sample’s surface.¹³

In order to fit the reflectivities taken when a potential was applied to the sample, the magnetization of the CoPd film was divided into two layers [CoPd layer “1” (film bulk) and “2” (surface), Fig. 6(a)] whose overall length and nuclear SLD were constrained to be that found for -0.02 V measurement. Previously, Weisheit *et al.*¹³ concluded the thickness of the organic layer (layer 3) was unchanged with electric field; therefore, we fixed the thickness and the SLD of the organic layer to be the same as that inferred from the -0.02 V measurement. The two adjustable parameters we optimized were the thickness of the layer 2 and its magnetic SLD. The best fit to the data was obtained for a magnetic surface (layer 2) thickness of $7.2(1)$ nm (Ref. 31) for applied potentials of -0.15 and -0.32 V. The magnetization of layer 2 was 904 ± 5 emu/cm³ ($\chi^2_\nu = 3.1$) and 920 ± 5 emu/cm³ ($\chi^2_\nu = 2.5$) for applied potentials of -0.15 V and -0.32 V, respectively [see Fig. 6(b)]. The estimation of the confidence bands for each curve showed that the confidence bands do not overlap at the high Q region [Fig. 5(a)]. For comparison, had the model for a uniform $M_0(z)$ been used to fit the data taken for these potentials, the values of χ^2_ν (or χ^2) would increase between 48% and 88%. We also investigated a model that allowed only the chemical profile of the magnetic layer to vary while its magnetization was constrained to be uniform. This model led to increases in χ^2_ν (or χ^2) by 42%. Therefore, the data taken for potentials of -0.15 and -0.32 V cannot be explained by either a model with uniform chemical and magnetization profiles (for the magnetic layer)

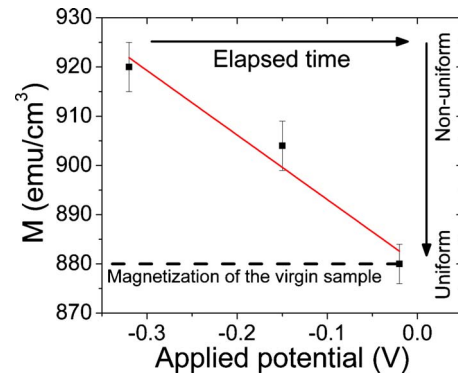


FIG. 7. (Color online) Magnetization of top 7.2 nm of CoPd film [layer 2 in Fig. 6(a)]. Elapsed time of the experiment and evolution of the magnetization are indicated. The magnetization inferred from the last measurement—one with an applied potential of -0.02 V—is statistically the same as the first measurement—one without an applied potential.

or by a model with a nonuniform chemical profile (for the magnetic layer) and uniform magnetization profile. The substantial improvement of χ^2 achieved using a nonuniform magnetization depth profile is compelling evidence for the influence of E field on the near-surface magnetization of the CoPd film. In particular, the magnetization of the surface region increases linearly with increasing magnitude of the negative applied potential (see Fig. 7). The largest applied potential $U = -0.32$ V corresponds to the electric field of about 10^8 V/m since the typical thickness of the insulating layer can be several nanometer. The approximately one part in 25 change in the surface magnetization with field is much larger than instrumental error that produce differences between R^+ and R^- , which range between one part in 200 to one part in 1000 for the neutron spectrometer.³²

It is important to note that our measurements were taken starting with the most negative potentials and ending with the least negative potential (see elapsed time arrow in Fig. 7). Had the magnetization been affected by a chemical attack on the sample during the measurements, one would expect the measurement taken last (-0.02 V) to show the most evidence for a change in the neutron-scattering length density profile compared to the virgin film. However, the chemical and magnetic scattering length density profile inferred from the last measurement ($U = -0.02$ V) for the CoPd film was *the most uniform and the most similar to the virgin film*. Thus, the simplest explanation for our observations is one that correlates a change in the magnetization depth profile with changes in the applied E field.

The thickness of the E -field-affected-magnetic layer, 7 nm, is comparable to the magnetic exchange (“healing”) length λ_0 (the characteristic length λ_0 over which a perturbation to one magnetic spin produces a perturbation in neighboring spins). For a wide range of ferromagnets λ_0 varies between 5 to 10 nm.³³ Future experiments could explore the relation between the thicknesses of the magnetically perturbed layer and the magnetic healing length using materials with different ratios of exchange stiffness to magnetization.

VI. CONCLUSIONS

In summary, we performed depth-resolved measurements of electric-field-induced changes in the saturation magnetization in a thin ferromagnetic film by polarized neutron reflectometry. Our measurements differ from earlier measurements, which have studied the influence of electric field on magnetic anisotropy. The change in the magnetization depth profile was achieved by applying a large electric field ($\sim 10^8$ V/m) to the sample's surface using an electrochemical potential. We showed that spin dependence of the neutron data could not be explained solely by a change in the chemical profile of the magnetic layer. However, the data could be explained solely by a change in the magnetization depth profile. The change to the magnetization was a linear function of modulus of the applied potential. The change took place in a region of the CoPd film closest to the surface that was at most 7.2 nm thick and was comparable to the magnetic healing length of the CoPd alloy. The magnetization of the remaining film was not affected.

Our result may be a manifestation of the spin-capacitor effect—the change in magnetization due to the accumulation

of spin-polarized charges close to the surface.¹⁷ In a ferromagnetic material, the electron DOS near the Fermi surface are spin polarized; thus, the net accumulation of charge due to the applied E field is also spin polarized.^{17,34} A perturbation to Fermi level may change the net magnetization accordingly. The results obtained in the present study provide quantitative information to test theoretical models of the magnetoelectric effect.

ACKNOWLEDGMENTS

We gratefully acknowledge discussions with D. Smith (LANL), N. Spaldin, and J. Rondinelli (UCSB). We thank Gerie Purdy (LANL) for performing ICP analysis of electrolyte solution. This work has benefited from the use of the Lujan Neutron Scattering Center at LANSCE, which is funded the Department of Energy's Office of Basic Energy Sciences. Los Alamos National Laboratory is operated by Los Alamos National Security LLC under DOE through Contract No. DE-AC52-06NA25396. E.E.F. was partially supported by DOE Award No. DE-SC0003678.

-
- ¹C. Chappert, A. Fert, and F. N. V. Dau, *Nature Mater.* **6**, 813 (2007).
- ²H. Ohno, D. Chiba, F. Matsukura, T. Omiya, E. Abe, T. Dietl, Y. Ohno, and K. Ohtani, *Nature (London)* **408**, 944 (2000).
- ³D. Chiba, M. Yamanouchi, F. Matsukura, and H. Ohno, *Science* **301**, 943 (2003).
- ⁴J. Hemberger, P. Lunkenheimer, R. Fichtl, H.-A. Krug von Nidda, V. Tsurkan, and A. Loidl, *Nature (London)* **434**, 364 (2005).
- ⁵N. Hur, S. Park, P. A. Sharma, J. S. Ahn, S. Guha, and S.-W. Cheong, *Nature (London)* **429**, 392 (2004).
- ⁶J. Van Den Boomgaard, D. R. Terrell, R. A. J. Born, and H. F. J. I. Giller, *J. Mater. Sci.* **9**, 1705 (1974).
- ⁷J. M. D. Coey, M. Venkatesan, and C. B. Fitzgerald, *Nature Mater.* **4**, 173 (2005).
- ⁸S. Zhang, *Phys. Rev. Lett.* **83**, 640 (1999).
- ⁹Y. B. Kudasov and A. S. Korshunov, *Phys. Lett. A* **364**, 348 (2007).
- ¹⁰I. V. Ovchinnikov and Kang L. Wang, *Phys. Rev. B* **78**, 012405 (2008).
- ¹¹Z. Tun, J. J. Noël, and D. W. Shoesmith, *J. Electrochem. Soc.* **146**, 988 (1999).
- ¹²D. G. Wiesler and C. F. Majkrzak, *Physica B* **198**, 181 (1994).
- ¹³M. Weisheit, S. Fähler, A. Marty, Y. Souche, Ch. Poinignon, and D. Givord, *Science* **315**, 349 (2007).
- ¹⁴M. Tsujikawa and T. Oda, *J. Phys.: Condens. Matter* **21**, 064213 (2009).
- ¹⁵H. Gleiter, J. Weissmueller, O. Wollersheim, and R. Wuerthshum, *Acta Mater.* **49**, 737 (2001).
- ¹⁶See special issue on double layer modeling: *Electrochim. Acta* **41** (14) (1996).
- ¹⁷J. M. Rondinelli, M. Stengel, and N. A. Spaldin, *Nat. Nanotechnol.* **3**, 46 (2008).
- ¹⁸J. M. Ziman, *Principles of the Theory of Solids*, 2nd ed. (Cambridge University Press, Cambridge, 1972), pp. 329–378.
- ¹⁹T. Maruyama, Y. Shiota, T. Nozaki, K. Ohta, N. Toda, M. Mizuguchi, A. A. Tulapurkar, T. Shinjo, M. Shiraishi, S. Mizukami, Y. Ando, and Y. Suzuki, *Nat. Nanotechnol.* **4**, 158 (2009).
- ²⁰J. A. Paulus, G. R. Parida, R. D. Tucker, and J. B. Park, *Biomaterials* **18**, 1609 (1997).
- ²¹Einar Bardal, in *Engineering Materials and Processes, Corrosion and Protection*, edited by B. Derby (Springer-Verlag, London, 2004).
- ²²G. P. Felcher, R. O. Hilleke, R. K. Crawford, J. Haumann, R. Kleb, and G. Ostrowski, *Rev. Sci. Instrum.* **58**, 609 (1987).
- ²³C. F. Majkrzak, *Physica B* **221**, 342 (1996).
- ²⁴M. R. Fitzsimmons and C. F. Majkrzak, in *Modern Techniques for Characterizing Magnetic Materials*, edited by Y. Zhu (Kluwer, Boston, 2005), pp. 107–152.
- ²⁵R. M. Richardson, J. R. P. Webster, and A. Zarbakhsh, *J. Appl. Crystallogr.* **30**, 943 (1997).
- ²⁶Since the potential values in Ref. 13 were nominal and no measurements versus a reference electrode were reported, a quantitative comparison of our results with those in Ref. 13 is not possible.
- ²⁷S. J. Blundell and J. A. C. Bland, *Phys. Rev. B* **46**, 3391 (1992).
- ²⁸L. G. Parratt, *Phys. Rev.* **95**, 359 (1954).
- ²⁹W. H. Press, B. P. Flannery, S. A. Teukolsky, and W. T. Vetterling, *Numerical Recipes in Fortran: The Art of Scientific Computation*, 2nd ed. (Cambridge University Press, Cambridge, 1992).
- ³⁰P. Patnaik, *Handbook of Inorganic Chemicals* (McGraw-Hill, New York, 2002).
- ³¹We also tested for correlation between these two parameters, by fixing the thickness of layer 2 in 1 nm steps and optimizing its magnetic SLD. With this approach we still found the optimum

layer thickness to be ~ 7 nm.

- ³²M. R. Fitzsimmons, B. J. Kirby, N. W. Hengartner, F. Trouw, M. J. Erickson, S. D. Flexner, T. Kondo, C. Adelman, C. J. Palmstrøm, P. A. Crowell, W. C. Chen, T. R. Gentile, J. A. Borchers, C. F. Majkrzak, and R. Pynn, [Phys. Rev. B **76**, 245301 \(2007\)](#).
- ³³R. Skomski, *Simple Models of Magnetism* (Oxford University Press, Oxford, 2008), p. 123.
- ³⁴N. A. Spaldin and R. Ramesh, *MRS Bull.* **33**, 1047 (2008).